Brief Report

Evaluating high-resolution computed tomography to study citrus tristeza virus-induced stem pitting

DJ Aldrich[1,2], R Bester[2], G Cook[3], A du Plessis[4], JT Burger[2], HJ Maree[2,5*]

[1]Agricultural Research Council, Infruitec-Nietvoorbij: Institute for Deciduous Fruit, Vines and Wine, Private Bag X5026, Stellenbosch 7599, South Africa; [2]Department of Genetics, Stellenbosch University, Private Bag X1, Matieland, 7602, South Africa; [3]Citrus Research International, P.O. Box 28, Nelspruit, 1200, South Africa; [4]Research group 3D Innovation, Stellenbosch University, Stellenbosch, South Africa; [5]Citrus Research International, P.O. Box 2201, Matieland, 7602, South Africa

*Correspondence to: hjmaree@sun.ac.za

Citation: Aldrich, D. J, Bester, R., Cook, G., du Plessis, A., Burger, J. T, & Maree, H. J. (2021). Evaluating high-resolution computed tomography to study citrus tristeza virus-induced stem pitting. Journal of Citrus Pathology, 8(1). http://dx.doi.org/10.5070/C481050093 Retrieved from https://escholarship.org/uc/item/4fw3c8pg

Abstract

Citrus tristeza virus (CTV) is the most important viral pathogen of citrus. CTV-induced stem pitting negatively impacts grapefruit and sweet orange production. The mechanisms of stem pitting development in CTV-infected citrus remain unclear. This study evaluated the utility of high-resolution computed tomography (CT) scanning as a tool to study stem pitting in live citrus material. CT scans were used to easily identify pits based on differences in tissue density. Stem pits were also mapped and modelled three-dimensionally along the length of the stem. High-resolution CT scanning proved to be a potentially valuable, non-destructive method for stem pitting characterization in citrus.

Keywords: CTV, X-ray tomography, 3D-modelling, Nano-CT, Micro-CT

Introduction

Citrus tristeza virus, a phloem-limited closterovirus in the family *Closteroviridae*, is the largest and most economically important RNA virus infecting citrus (Moreno et al., 2008; Fuchs et al., 2020). The complex interactions of CTV with its various citrus hosts result in one of three disease phenotypes, namely quick decline (tristeza), stem pitting and seedling yellows (Moreno et al., 2008; Albiach-Marti, 2013). Citrus tristeza virus induces severe stem pitting in susceptible citrus hosts, including grapefruit and sweet orange, that was focused on in this study (Dawson et al., 2013). Citrus growing areas affected by severe stem pitting isolates of CTV can only remain productive through mild strain cross-protection programs, or by avoiding planting susceptible citrus varieties (Dawson et al., 2013). Mild-strain cross protection of citrus against severe-pitting CTV has been particularly effective in Brazil ('Pera' sweet orange), South Africa (Star Ruby and Marsh grapefruit), Australia and Peru (Folimonova et al., 2020). Stem pitting is thought to result from an interference with normal cambium development and differentiation, thereby negatively affecting stem growth (Dawson et al., 2013). Brlansky et al. (2002) postulated that stem pitting development in CTV infection is likely the result of impaired xylem production in the affected sites. The characteristic stem pits appear in areas with developmental disruption, where areas surrounding these sites grow normally, leaving the afflicted areas as indented pits (Tatineni and Dawson, 2012; Dawson et al., 2013). There are a spectrum of distinct phenotypes of stem pitting in citrus, ranging from older trees exhibiting large pits that are visible without removing the bark layer, to others that show a high density of smaller pits, referred to as "cheesy bark" or "honey-comb" (Moreno and Garnsey, 2010; Dawson et al., 2013; Cook et al., 2016). Stem pitting restricts carbohydrate transport, causing stunted growth and reduced fruit size and quality (Hilf et al., 2007; Dawson et al., 2013). Even though stem pitting is a common virus-induced disease symptom in woody perennials, the determinants for stem pitting development in citrus remain unclear (Dawson et al., 2013; Cook et al., 2016). In a recent study we discovered that CTV strains with minor nucleotides differences had significantly different stem pitting responses on grapefruit (Cook et al., 2020).

Studying CTV-induced stem pitting has several experimental constraints. Stem pits take months to develop following experimental inoculation (Tatineni and Dawson, 2012) and are usually only visible after removing the bark layer in test plants. Additionally, the occurrence and severity of stem pitting when different strains of CTV infect different citrus species vary substantially (Dawson et al., 2013), making symptom expression difficult to predict. The destructive sampling necessary to identify and further characterize stem pits is potentially a limiting factor and

also forgoes the possibility of tracking early stem pitting development in time-course experiments. A non-destructive method of visualizing and characterizing stem pits could therefore be a valuable tool for studying virus-induced stem pitting and facilitate experimental design and execution.

Computed Tomography (CT) scanning technology was established in the 1970s and used extensively in the field of Medicine as a non-destructive diagnostic tool in the form of Computerized Axial Tomography (CAT) scanners (Staedler et al., 2013; Du Plessis et al., 2016). In subsequent decades the applications of X-ray CT expanded beyond the medical realm into broader research and industrial applications, giving rise to the term 'industrial CT', referring to non-medical applications of the technology (Du Plessis et al., 2017). The basic principles of the scanning process involve exposing an object to collimated X-rays, after which the absorbed radiation is detected on the opposing side of the X-ray source by a detector. This is repeated thousands of times from varying angles around the sample, providing a mass of two-dimensional radiographic projection images to be reconstructed into a full, three-dimensional rendering of the sample (Masschaele, 2007; Du Plessis et al., 2016, 2017; Ham et al., 2017). CT scanning allows the detection of minute differences in tissue density and provides a non-destructive analysis and quantification tool for a wide variety of materials (Staedler et al., 2013; Du Plessis et al., 2016; Kampschulte et al., 2016; Ham et al., 2017; Du Plessis et al., 2017).

X-ray CT technology has improved significantly over time, owing to enhanced computing power and technological advancements in hardware and software development (Du Plessis et al., 2016; Kampschulte et al., 2016; Ham et al., 2017). The term microcomputed tomography (micro-CT) has since been introduced and loosely refers to CT scanning at resolutions of 100 micrometer (⌈m) or less, with the average range suggested to be 5 to 50 ⌈m (Kampschulte et al., 2016). Further improvement of micro-CT technology produced the nano-CT systems, capable of sub-micrometer resolution scanning (Masschaele, 2007; Du Plessis et al., 2016; Kampschulte et al., 2016). CT scanning at these resolutions is often also referred to under the umbrella-term; high-resolution computed tomography (HRCT) scanning (Brodersen et al., 2011, 2010). HRCT scanning is increasingly being utilized in a wide variety of research fields, including biological sciences (Mizutani and Suzuki, 2012), geosciences (Cnudde and Boone, 2013), materials sciences (Maire and Withers, 2014) and food sciences (Schoeman et al., 2016).

In this study we investigated the usefulness of HRCT, by means of nano-CT scanning, as a tool to characterize stem pitting in citrus. We set out to determine the image quality and resolution achievable for citrus samples, the ease with which stem pits could be identified compared to surrounding plant tissue and the capacity of the appropriate software to visualize and analyze our data.

Materials and Methods

Plant material and greenhouse conditions

Citrus tristeza virus infected material was obtained from grapefruit plants (*Citrus* Osb. × *paradisi* (Macfad.)) cv. 'Star Ruby' and 'Marsh' that were established on 'Carrizo' citrange (*C.* × *sinensis* × *Poncirus trifoliata* L.Raf.) rootstocks and maintained in a climate-controlled greenhouse. Plants were bark-inoculated in late-2016 with CTV genotype T3 from a sweet orange (*C.* × *sinensis*) source plant. Greenhouse growing conditions included natural light, with temperatures ranging between 22 °C and 28 °C. Side shoots were continuously removed, and plants pruned yearly. Sections of grapefruit stems (±6 months old), roughly 4 cm in length, suspected to include stem pits were sampled in mid-2018 in each case. The bark layer was retained on all stem sections to serve as a proxy for live/growing material, and to allow imaging of both phloem and xylem tissue.

Sample preparation, CT scanning and data analysis

Citrus stem samples were imaged via nano-CT scanning at the CT Scanner Facility (Du Plessis et al., 2016) of the Central Analytical Facilities (CAF) of Stellenbosch University. CT scans were performed using the Nanotom S model nano-CT scanner (General Electric Sensing and Inspection Technologies/Phoenix X-ray, Wunstorff, Germany).

Samples were scanned at resolutions between 5 and 6 ⌈m. In all instances the stem sections were multi-scanned, in 5 to 7 scans depending on sample length, and stitched together during reconstruction. The X-ray settings were 80 kV; 200 µA (no beam filter used) with a voxel size of 5 ⌈m. The image acquisition time was set to 500 milliseconds per image at 3000 instances during a continuous 360-degree rotation of the sample in the scanner. Image reconstruction was performed using the system supplied Datos reconstruction software. Reconstruction was performed with no beam hardening correction and automatic geometry correction, in multiscan reconstruction mode to automatically stitch together the 5-7 scans into one large volume data set for each sample. Analysis and visualization were performed using Volume Graphics VGStudioMax 3.3 (Volume Graphics, Heidelberg, Germany). The data was contrasted appropriately using a linear gradient covering the greyscale histogram peak of the material, and cross-sectional images evaluated visually. Segmentation was performed in a slice-by-slice manner to identify the regions of interest using the drawing tool (manually) and subsequently visualized using a 3D isosurface rendering.

Results

We first evaluated the quality of images that could be generated. Figure 1 illustrates the high resolution and image quality achieved using the nano-CT scanner. The Volume Graphics VGStudioMax 3.3 software allowed clear, interactive visualization of the citrus stems in three dimensions. The software also provided a reference model of the whole sample as shown in Fig. 1 and Fig. 2, which indicated axes and the position of the view pane along the length of the sample, in real-time.

The next objective was to identify stem pits based on the imaging principles of the X-ray CT scanner. As shown in Fig. 1, the stem pits (arrows) are clearly distinguishable in a transverse section as light-gray, triangular shapes, observed due to density differences compared to normally differentiated tissue surrounding these areas. The unorganized mass of cells at the cambial interface in pitted areas is also apparent and is distinguishable from the surrounding, normal tissue.

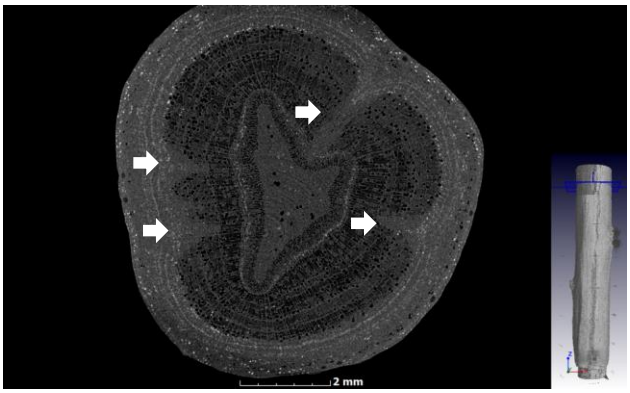

Fig. 1. Transverse section of nano-CT scan showing stem pits and affected xylem tissue (indicated by white arrows) extending inwards toward the pith of the citrus stem. Insert (bottom right corner) shows the whole sample with the relative position of the transverse section.

Longitudinal sections of the affected citrus stem were generated to observe pitted tissue along the length of the sample. Fig. 2 shows differences in tissue density and stem morphology between pitted and unpitted sections of the stem. The conical, wedge-like morphology of the pits was also apparent from the longitudinal perspective.

Furthermore, three-dimensional (3D) imaging of stem pit morphology and formation along the stem was investigated. A 3D modelled image of pitted areas was mapped as shown in Fig. 3. A cross-sectional video could be generated as the software panned across the length of the sample along the z-axis, providing a unique perspective as to how the shape and size of the stem pits change along the length of the sample, and how these changes relate to alterations in the shape and diameter of the stem. A cross-sectional video is provided under supplementary material 1 (S1).

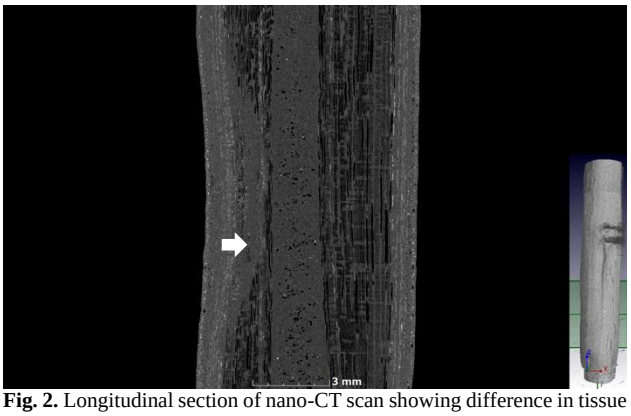

Fig. 2. Longitudinal section of nano-CT scan showing difference in tissue density between pitted (left of the central pith - indicated by white arrow) and unpitted (right of the central pith) portions of the citrus stem. Insert (bottom right corner) shows the whole sample with the relative position of the longitudinal section.

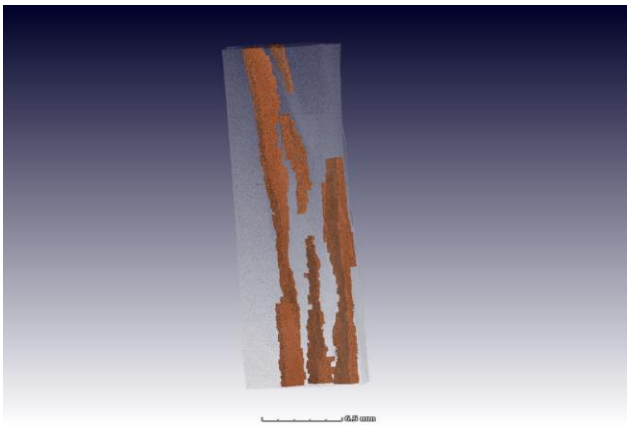

Fig. 3. A three-dimensional model of a citrus stem with stem pits mapped in red along the length of the sample.

Discussion

This proof-of-concept study illustrated the utility of X-ray CT to study CTV-induced stem pitting in citrus. The high-resolution images produced by the nano-CT scanner (Fig. 1 and 2) allowed clear identification of stem pits. Sampling, scanning, data reconstruction and collection as shown here could be performed in under 8 hours, allowing for a same-day experimental design. For smaller regions of interest (e.g. at one pitting site) it is possible to do this in 1 to 2 hours. These scans also illustrated the unexpectedly large area of xylem tissue affected by stem pitting in each case. The impacted tissue extended inward substantially from the interface of xylem and phloem material, where the stem pits manifest externally. The normal ring of cambial tissue was also not visible at these pitted sites (Fig. 1), which is consistent with previous findings of CTV-induced stem pitting (Brlansky et al., 2002). The graphical representation illustrated in Figure 3 serves as one example

of many possible ways in which the VGStudioMax 3.3 software could be applied to further analyze the X-ray CT data, to suit a specific investigation. The time required to perform such additional analyses will vary depending on the intended application, but generally can be completed within a few hours. The software allowed convenient visualization of data and provided a unique perspective by enabling one to pan along the length of the sample, viewing one cross-section at a time. In plant systems, this would be equivalent to data otherwise only obtainable from fixing and serial sectioning (van der Niet et al., 2010; Staedler et al., 2013; Ham et al., 2017).

There are many possible applications of HRCT to complement stem pitting characterization in citrus. It can be employed as a pre-screen for stem pitting development before destructive sampling and testing is carried out for example. This has the potential to save time, considering the months needed for stem pits to develop in test material following experimental inoculation (Tatineni and Dawson, 2012). The X-ray CT data can also facilitate selection of stem-sections to sample for a specific investigation. As an example, this approach can be useful for embedding, sectioning and microscopy trials by demarcating areas of severe pitting for further characterization. The non-destructive nature of the imaging process, and the ease of sample preparation (Du Plessis et al., 2017) makes HRCT scanning an ideal complementary analysis tool to existing methods.

Given the spectrum of distinct stem pitting phenotypes produced from different citrus-CTV interactions (Dawson et al., 2013), it would be of interest to graphically map the 3D morphology of pits in each case. This would be even more effective when defined stem pitting phenotypes can be induced in test material. Tatineni and Dawson (2012) demonstrated differences in stem pitting severity in *C. macrophylla* and Mexican lime plants infected with different deletion mutants of a CTV infectious clone. This study yielded useful resources for further analysis by establishing defined stem pitting phenotypes induced by defined CTV mutants. The incorporation of a GFP reporter gene in these infectious clones also provided valuable insights into the aberrant virus localization of CTV in cases of severe pitting (Tatineni and Dawson, 2012). This also provided the opportunity to incorporate fluorescence microscopy into the suite of tools available for characterizing CTV-induced stem pitting in citrus.

Software tools available for analyzing HRCT scanning data could further be applied to allow statistical testing of differences in plant tissue characteristics under various conditions. The use of HRCT was effectively utilized for quantifying plant material properties at different growth stages, tissue development and damage and stress effects (Heeraman et al., 1997; Pierret et al., 1999; Han et al., 2008; Guelpa et al., 2016; Lindgren et al., 2016). The addition of quantitative data to tissue damage caused by different stem pitting phenotypes would be a useful contribution to understanding their effects on tree health and could inform subsequent studies.

Another application would be to track stem pitting development in growing material over time. To that end, it is possible to accommodate whole plants in a micro-CT scanner, although the resolution would be slightly less than that achievable with nano-CT. In theory the same resolution is technically feasible but practically the size of a living plant combined with the hardware size constraints limits the application for whole plants to 10 to 20 ⌈m. The success of such scans is dependent on the size and dimensions of the plant as material is required to be centered and in-frame during revolutions in the scanner. Du Plessis et al. (2016, 2017) outline several parameters for consideration when using HRCT scanning for application in biological sciences, including spatial limitations and the effects of sample size on resolution.

High resolution CT scanning is fast becoming a valuable, widely used technology for a broad spectrum of research fields. From its initial applications in the realm of plant sciences for studying root development (Heeraman et al., 1997), its application has expanded to include studies aimed at quantifying wood moisture content (Lindgren et al., 2016), assessing stem-boring beetle damage (Lyons et al., 2020) and measuring density properties of maize kernels (Guelpa et al., 2016). The application of HRCT scanning to study virus-induced disease phenotypes in woody perennials, however, has not been extensively used. This technology provides a unique tool to investigate CTV-induced stem pitting in citrus.

Acknowledgments

The authors would hereby like to thank the personnel at the CT Scanner Facility at Stellenbosch University, especially Mr. Stephan le Roux and Ms. Muofhe Tshibalanganda, for their excellent and friendly service. The authors thank the Citrus Growers' Association of Southern Africa (CGA) and Citrus Research International (CRI) for funding CRI project 1160. We would also like to thank the National Research Foundation (NRF) for their financial assistance towards this research. Opinions expressed and conclusions arrived at, are those of the authors and are not necessarily to be attributed to the NRF.

References

Albiach-Marti, M.R., 2013. The Complex Genetics of Citrus tristeza virus, in: Romanowski, V. (Ed.), Current Issues in Molecular Virology - Viral Genetics and Biotechnological Applications. InTech. https://doi.org/10.5772/56122.

Brlansky, R.H., Howd, D.S., Broadbent, P., Damsteegt, V.D., 2002. Histology of sweet orange stem pitting caused by an Australian isolate of Citrus tristeza virus. Plant Dis. 86, 1169–1174. https://doi.org/10.1094/PDIS.2002.86.10.1169.

Brodersen, C.R., Lee, E.F., Choat, B., Jansen, S., Phillips, R.J., Shackel, K.A., McElrone, A.J., Matthews, M.A., 2011. Automated analysis of three-dimensional xylem networks using high-resolution computed tomography.

New Phytol. 191, 1168–1179. https://doi.org/10.1111/j.1469-8137.2011.03754.x.

Brodersen, C.R., McElrone, A.J., Choat, B., Matthews, M.A., Shackel, K.A., 2010. The Dynamics of Embolism Repair in Xylem: In Vivo Visualizations Using High-Resolution Computed Tomography. Plant Physiol. 154, 1088–1095. https://doi.org/10.1104/pp.110.162396.

Cnudde, V., Boone, M.N., 2013. High-resolution X-ray computed tomography in geosciences: A review of the current technology and applications. Earth-Sci. Rev. 123, 1–17. https://doi.org/10.1016/j.earscirev.2013.04.003.

Cook, G., van Vuuren, S.P., Breytenbach, J.H.J., Steyn, C., Burger, J.T., Maree, H.J., 2016. Characterization of Citrus tristeza virus Single-Variant Sources in Grapefruit in Greenhouse and Field Trials. Plant Dis. 100, 2251–2256. https://doi.org/10.1094/PDIS-03-16-0391-RE.

Cook, G., Coetzee, B., Bester, R., Breytenbach, J.H.J., Steyn, C., de Bruyn, R., Burger, J.T., Maree, H.J., 2020. Citrus Tristeza Virus Isolates of the Same Genotype Differ in Stem Pitting Severity in Grapefruit. Plant Dis. 104, 2362–2368. https://doi.org/10.1094/PDIS-12-19-2586-RE.

Dawson, W.O., Garnsey, S.M., Tatineni, S., Folimonova, S.Y., Harper, S.J., Gowda, S., 2013. Citrus tristeza virus-host interactions. Front. Microbiol. 4. https://doi.org/10.3389/fmicb.2013.00088.

Du Plessis, A., Broeckhoven, C., Guelpa, A., le Roux, S.G., 2017. Laboratory x-ray micro-computed tomography: a user guideline for biological samples. GigaScience 6. https://doi.org/10.1093/gigascience/gix027.

Du Plessis, A., le Roux, S.G., Guelpa, A., 2016. The CT Scanner Facility at Stellenbosch University: An open access X-ray computed tomography laboratory. Nucl. Instrum. Methods Phys. Res. Sect. B Beam Interact. Mater. At. 384, 42–49. https://doi.org/10.1016/j.nimb.2016.08.005.

Folimonova, S.Y., Achor, D., Bar-Joseph, M., 2020. Walking Together: Cross-Protection, Genome Conservation, and the Replication Machinery of Citrus tristeza virus. Viruses 12, 1353. https://doi.org/10.3390/v12121353.

Fuchs, M., Bar-Joseph, M., Candresse, T., Maree, H.J., Martelli, G.P., Melzer, M.J., Menzel, W., Minafra, A., Sabanadzovic, S., Report Consortium, I., 2020. ICTV Virus Taxonomy Profile: Closteroviridae. J. Gen. Virol. 101, 364–365. https://doi.org/10.1099/jgv.0.001397.

Guelpa, A., Du Plessis, A., Manley, M., 2016. A high-throughput X-ray micro-computed tomography (μCT) approach for measuring single kernel maize (Zea mays L.) volumes and densities. J. Cereal Sci. 69, 321–328. https://doi.org/10.1016/j.jcs.2016.04.009.

Ham, H., Du Plessis, A., le Roux, S.G., 2017. Microcomputer tomography (microCT) as a tool in Pinus tree breeding: pilot studies. N. Z. J. For. Sci. 47, 2. https://doi.org/10.1186/s40490-016-0084-9.

Han, L., Dutilleul, P., Prasher, S.O., Beaulieu, C., Smith, D.L., 2008. Assessment of Common Scab-Inducing Pathogen Effects on Potato Underground Organs Via Computed Tomography Scanning. Phytopathology® 98, 1118–1125. https://doi.org/10.1094/PHYTO-98-10-1118.

Heeraman, D.A., Hopmans, J.W., Clausnitzer, V., 1997. Three dimensional imaging of plant roots in situ with X-ray Computed Tomography. Plant Soil 189, 167–179. https://doi.org/10.1023/B:PLSO.0000009694.64377.6f

Hilf, M.E., Garnsey, S.M., Robertson, C., Gowda, S., Satyanarayana, T., Irey, M., Sieburth, P., Dawson, W.O., 2007. Characterization of recently introduced HLB and CTV isolates. Proc. Fla. State Hort. Soc. 120, 138-141.

Kampschulte, M., Langheinirch, A., Sender, J., Litzlbauer, H., Althöhn, U., Schwab, J., Alejandre-Lafont, E., Martels, G., Krombach, G., 2016. Nano-Computed Tomography: Technique and Applications. RöFo - Fortschritte Auf Dem Geb. Röntgenstrahlen Bildgeb. Verfahr. 188, 146–154. https://doi.org/10.1055/s-0041-106541.

Lindgren, O., Seifert, T., Du Plessis, A., 2016. Moisture content measurements in wood using dual-energy CT scanning – a feasibility study. Wood Mater. Sci. Eng. 11, 312–317. https://doi.org/10.1080/17480272.2016.1201863.

Lyons, C.L., Tshibalanganda, M., Plessis, A.D., 2020. Using CT-scanning technology to quantify damage of the stem-boring beetle, Aphanasium australe, a biocontrol agent of Hakea sericea in South Africa. Biocontrol Sci. Technol. 30, 33–41. https://doi.org/10.1080/09583157.2019.1682518.

Maire, E., Withers, P.J., 2014. Quantitative X-ray tomography. Int. Mater. Rev. 59, 1–43. https://doi.org/10.1179/1743280413Y.0000000023.

Masschaele, B., 2007. High resolution computed tomography at the Ghent University: measuring, visualizing and analyzing the internal structure of objects with sub-micron precision. Proceedings of Science, 046, 1–8. https://lib.ugent.be/catalog/pug01:426840.

Mizutani, R., Suzuki, Y., 2012. X-ray microtomography in biology. Micron 43, 104–115. https://doi.org/10.1016/j.micron.2011.10.002.

Moreno, P., Ambros, S., Albiach-Martí, M.R., Guerri, J., Pena, L., 2008. Citrus tristeza virus: a pathogen that changed the course of the citrus industry. Mol. Plant Pathol. 9, 251–268. https://doi.org/10.1111/j.1364-3703.2007.00455.x.

Moreno, P., and Garnsey, S. M., 2010. Citrus tristeza diseases - A worldwide perspective. Pages 27-49 in: Citrus tristeza virus Complex and Tristeza diseases. Karasev, A., and Hilf, M. E., eds. The American Phytopathological Society, St. Paul, MN.

Pierret, A., Capowiez, Y., Moran, C.J., Kretzschmar, A., 1999. X-ray computed tomography to quantify tree

rooting spatial distributions. Geoderma 90, 307–326. https://doi.org/10.1016/S0016-7061(98)00136-0.

Schoeman, L., Du Plessis, A., Manley, M., 2016. Non-destructive characterisation and quantification of the effect of conventional oven and forced convection continuous tumble (FCCT) roasting on the three-dimensional microstructure of whole wheat kernels using X-ray micro-computed tomography (μCT). J. Food Eng. 187, 1–13. https://doi.org/10.1016/j.jfoodeng.2016.04.015.

Staedler, Y.M., Masson, D., Schönenberger, J., 2013. Plant Tissues in 3D via X-Ray Tomography: Simple Contrasting Methods Allow High Resolution Imaging. PLoS ONE 8, e75295. https://doi.org/10.1371/journal.pone.0075295.

Tatineni, S., Dawson, W.O., 2012. Enhancement or Attenuation of Disease by Deletion of Genes from Citrus Tristeza Virus. J. Virol. 86, 7850–7857. https://doi.org/10.1128/JVI.00916-12.

Tatineni, S., Robertson, C.J., Garnsey, S.M., Dawson, W.O., 2011. A plant virus evolved by acquiring multiple nonconserved genes to extend its host range. Proc. Natl. Acad. Sci. 108, 17366–17371. https://doi.org/10.1073/pnas.1113227108.

Van der Niet, T., Zollikofer, C.P.E., León, M.S.P. de, Johnson, S.D., Linder, H.P., 2010. Three-dimensional geometric morphometrics for studying floral shape variation. Trends Plant Sci. 15, 423–426. https://doi.org/10.1016/j.tplants.2010.05.005.